Bulgarian Chemical Communications, Volume 55, Issue 3 (pp. 367-372) 2023 DOI: 10.34049/bcc.55.3.SIMNS06

Time-harmonic nano-cracks interaction in functionally graded piezoelectric half-plane

Ts. Rangelov[1]*, P. Dineva[2]

[1]*Institute of Mathematics and Informatics, BAS, Acad. G. Bonchev Str., Bl. 8, 1113 Sofia, Bulgaria*
[2]*Institute of Mechanics, BAS, Acad. G. Bonchev Str., Bl. 4, 1113 Sofia, Bulgaria*

Received: June10, 2023; Revised: July 16, 2023

A system of two nano-cracks situated in an exponentially graded in depth piezoelectric material (PEM) half-plane under time-harmonic anti-plane load is studied. The mechanical model is in the frame of 2D elastodynamics for graded continua and surface elasticity theory of Gurtin and Murdoch (GM). Mathematical model is defined by a system of integro-differential equations along the crack lines. The computational tool is an efficient nonhypersingular traction boundary integral equation method (BIEM) based on the analytically derived Green's function for the graded half-plane. The obtained results are with important application in computational nano-mechanics and in engineering practice concerning the reliability of the micro-electro-mechanical-systems emerged to meet the requirements of miniaturization and integration of different types of electronic components.

Keywords: Graded PEM half-plane; Nano-cracks; Anti-plane wave; GM surface elasticity; BIEM; Stress concentration

INTRODUCTION

There is a general agreement concluded from the experiments that the properties of piezoelectric nano-materials are size-dependent. For example: (a) as the nano-wire diameter decreases from 80 nm to 20 nm, the Young's modulus of ZnO nano-wire increases from 140 to 160 GPa (Agrawal *et al.* [1]); (b) the fracture strength of ZnO nano-wires increases as the nano-wire diameter decreases (Xu *et al.* [2]); (c) the piezoelectric constants of GaN nano-wires were reported up to six times more than that of the bulk values (Minary-Jolandan *et al.* [3]). The classical continuum mechanics is incapable to capture the size-dependence of solids behavior as the intrinsic length scale is not present in the constitutive laws. As a result, many non-classical theories were developed to study the size-dependent mechanical problems. A categorization of the nano-mechanical models depending on the link between material microstructure and intrinsic length scale h is presented by Manolis *et al.* [4]. Continuum mechanics-based models ($h \approx 10^{-2} m$) for nano-objects are non-local elasticity, strain gradient theory and surface elasticity model (Gurtin-Murdoch [5]). In the latter model, the surface is regarded as a thin layer with negligible thickness adhered to the underlying bulk material without slipping. The surface properties and constitutive relations are different from those of the bulk. Despite its zero thickness, the surface layer S is otherwise elastic, isotropic with its own surface Lame constants λ^S, μ^S and local constitutive law written in tangential direction l such as $\sigma_{ll}^S = \left(\lambda^S + 2\mu^S\right)\varepsilon_{ll}^S$, where σ_{ll}^S and ε_{ll}^S are the tangential stress and strain, correspondingly. Thus, under the Gurtin-Murdoch theory, the traditional boundary conditions along the surface layer S are replaced by non-classical ones that account for the unconventional surface elasticity conditions, while the bulk materials can still be described by classical continuum theory.

The main aim of the current work is to model the dynamic behavior of two nano-cracks in an exponentially graded in depth PEM half-plane under time-harmonic SH-wave. For numerical results we proceed with non-hypersingular traction BIEM using the half-plane Green's function analytically derived in [6].

MECHANICAL MODEL

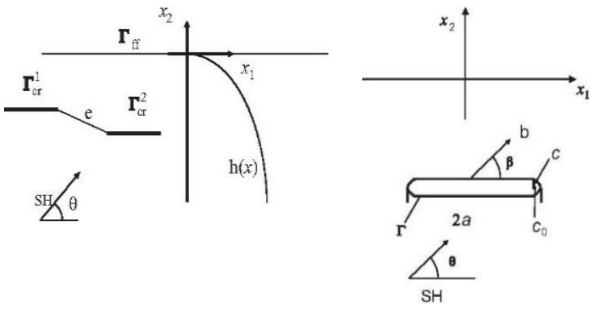

(a) (b)

Fig. 1. a) Two nano-cracks in functionally graded half-plane; b) Reference model of a single blunt nano-crack.

In a Cartesian coordinate system $Ox_1x_2x_3$ a piezoelectric half-plane $R_-^2 = \{x = (x_1, x_2), x_2 < 0\}$ is considered poled in x_3 - direction and subjected

* To whom all correspondence should be sent:
E-mail: rangelov@math.bas.bg

to time-harmonic incident SH-wave with frequency ω. The only non-vanishing displacements are the anti-plane mechanical displacement $u_3(x,\omega)$ and the in-plane electrical displacements $D_i(x,\omega)$, $i = 1,2$.

Let us introduce the notations for the generalized displacements, stresses and density as follows:

$$u_K(x,\omega) = \big(u_3(x,\omega), \phi(x,\omega)\big),$$
$$\sigma_{iJ}(x,\omega) = C_{iJKl}(x)u_{K,l}(x,\omega)$$
$$\rho_{JK}(x) = \rho(x),$$

where $\rho(x) = \rho^0 h(x)$ is the variable density for $J = K = 3$ and $\rho_{JK}(x) = 0$ for $J = 4$ or $K = 4$; $\phi(x,\omega)$ is the electric potential.

The equation of motion in the absence of body forces and free volume charges is:

$$\sigma_{iJ,i}(x,\omega) + \rho_{JK}(x)\omega^2 u_K(x,\omega) = 0 \qquad (1)$$

where:

$C_{i33l}(x) = c_{44}(x)$, $C_{i34l}(x) = e_{15}(x)$ and $C_{i44l}(x) = -\varepsilon_{11}(x)$ in the case of $i = l$ and all three generalized material characteristics are zero at $i \neq l$.

Note that $c_{44}(x) = c_{44}^0 h(x)$, $e_{15}(x) = e_{15}^0 h(x)$ and $\varepsilon_{11}(x) = \varepsilon_{11}^0 h(x)$ are the shear stiffness, piezoelectric and dielectric permittivity of the graded PEM. The exponential inhomogeneity function $h(x) = e^{2bx_2}$ is with coefficient b and $c_{44}^0, e_{15}^0, \varepsilon_{11}^0, \rho^0$ are the reference constants.

The boundary condition along the free surface is:

$$t_J = \sigma_{iJ}(x,\omega)n_i(x) = 0 \qquad (2)$$

where $n_i(x)$ is the outward normal vector.

Following the Gurtin-Murdoch model [5], the boundary condition for the mechanical stresses along the crack's line l is:

$$t_3(x,\omega) = -\mu^S \frac{\partial^2 u_3}{\partial l^2}, \qquad (3)$$

where μ^S is the shear modulus of the infinitely thin surface layer S between the crack and matrix. Both nano-cracks are electrically impermeable, i.e., $D_n(x,\omega) = 0$ for $x \in S$.

The total wave field in the graded PEM half-plane is a sum of the free-field wave motion displacements u_K^{ff} and tractions t_K^{ff} and the scattered by the cracks ones u_K^{sc}, t_K^{sc}. The free-field wave displacement and traction in the graded half-plane is the wave motion in the cracks' free half-plane. It is a sum of the incident waves and the reflected ones by the traction-free half-plane boundary. Analytically derived solution for the free-field wave motion is presented in [6].

The mechanical model is presented by the governing equation (1) and the boundary conditions discussed above.

The aim is to obtain solutions for frequency-dependent displacements, strains and stresses in the graded PEM half-plane. In addition, stress concentration fields near the nano-cracks are evaluated. The computational tool used for solution of this boundary-value problem (BVP) is an efficient non-hypersingular traction BIEM based on analytically derived Green's function for exponentially graded piezoelectric half-plane. The applied BIEM based on the fundamental solution for graded PEM full plane is described and verified in [7]. The innovative element here is the solution of dynamic fracture problem for multiple nano-cracks in a graded PEM half-plane with BIEM based on the Green's function.

NUMERICAL RESULTS

The numerical scheme for solution of the BVP under consideration is based on discretization and collocation technique. The mesh employed for each nano-crack with half-length $a = 2.5x10^{-9}m$ and curvature radius $c = 0.375\,a$ consists of 10 quadratic boundary elements (BEs), 8 BEs along the flat part of the crack's boundary Γ denoted by $\Gamma^+ \cup \Gamma^-$ and 2 BEs along the semi-elliptic left and right parts of Γ denoted as Γ^l and Γ^r correspondingly. Quarter-point BEs for correctly modelling the crack-tip zones where the asymptotic generalized displacement behavior as $O(\sqrt{r})$ at $r \to 0$ are used.

After discretization of the system of non-hypersingular traction BIEs an algebraic system of equations with respect to the generalized displacements along the cracks' surfaces is obtained and solved. The displacements and strain-stress state at any point of the graded half-plane can be determined by the usage of the well-known integral representation formulae, see [7]. The numerical scheme is realized by the verified code basing on Mathematica software, see [8]. The following dimensionless parameters are introduced:

(a) Surface parameter $s = \mu^S / 2c_{44}^0\, cc_s$, where $\mu^S = \pm 6.091 N/m$ is taken from [9]. The notation c_s is used in order to decrease or increase the fixed value of the curvature radius c of the semi-elliptic nano-crack root. The value of the surface parameter decreases/increases with increase/decrease of the curvature radius c. In the case $\mu^S = 0$, the surface parameter $s = 0$ and the non-classical boundary conditions recover the classical ones;

(b) Dimensionless frequency defined as:

$$\Omega = a\omega \sqrt{\frac{\rho^0}{c_{44}^0 + \frac{(e_{15}^0)^2}{\varepsilon_{11}^0}}};$$

(c) Dimensionless inhomogeneity magnitude defined as $\beta = 2a|b|$. The reference material is PZT-4 with the following material properties:

$c_{44}^0 = 2.5 \times 10^{10}\, N/m^2$; $e_{15}^0 = 12.7\, C/m^2$; $\varepsilon_{11}^0 = 64.6 \times 10^{-10}\, C/V.m$; $\rho^0 = 7500\, kg/m^3$.

The normalized stress concentration factor (SCF) F_{III}^* and electrical field concentration factor (EFCF) F_E^* close to the blunt nano-crack-tip at the point $(\pm x_1, 0)$ are evaluated by the formulae:

$$F_{III}^*\big((\pm x_1, 0), \omega\big) = \frac{\sigma_{23}\big((\pm x_1,0),\omega\big)}{\sigma\sqrt{\pi a}}\sqrt{2\pi(x_1 \mp a)}, \quad |x_1| > a; \tag{4}$$

$$F_E^*\big((\pm x_1, 0), \omega\big) = e_{15}^0 \frac{E_3\big((\pm x_1,0),\omega\big)}{\sigma\sqrt{\pi a}}\sqrt{2\pi(x_1 \mp a)}, \quad |x_1| > a. \tag{5}$$

where:

$$E_3 = \frac{\sigma_{24}\big((\pm x_1,0),\omega\big)c_{44}^0 - \sigma_{23}\big((\pm x_1,0),\omega\big)e_{15}^0}{c_{44}^0\varepsilon_{11}^0 + \big(e_{15}^0\big)^2};$$

$$\sigma = \underset{S}{max}\sqrt{\big(\sigma_{23}^{in}\big)^2 + \big(\sigma_{24}^{in}\big)^2}.$$

What follows is a parametric study shown by Figures 2-6. All the figures illustrate the sensitivity of both the mechanical and electrical concentration fields near the nano-cracks on the following factors:

(a) The frequency of the incident wave and the value of the resonance frequency;

(b) The geometry of the nano-cracks configuration - collinear, parallel or shifted cracks;

(c) The influence of the half-plane boundary when compare Figs. 2a, 3a and Figs. 2b, 3b;

(d) The surface elasticity phenomenon: the dynamic response decreases with increase of the positive surface elasticity parameter and increases with the negative surface elasticity parameter. This happens because of destruction and reorganization of the atom symmetry along the interfaces at nano-level.

The size of the crack has strong influence on the scattered and diffraction wave field and also on the local zones of stress and electrical field concentrations. With decreasing of the crack size, surface elasticity phenomena arise and *vice versa* - cracks with size at macro-level do not show surface elasticity properties. Normalized displacement amplitude $|u_3|$ along the free surface of the PEM graded half-plane is presented in Fig. 6 for the following fixed data: inhomogeneity magnitude is $\beta = 0.2$, surface elasticity parameter is $s = 0.02$, separate distance between both nano-cracks is $e = 0.5a$, embedded depth is $d = a$, normalized frequencies of the incident normal SH wave are Ω=1.1; 1.3; 1.7.

Two different crack configuration geometries were studied, namely: (a) two collinear nano-cracks; (b) two shifted nano-cracks.

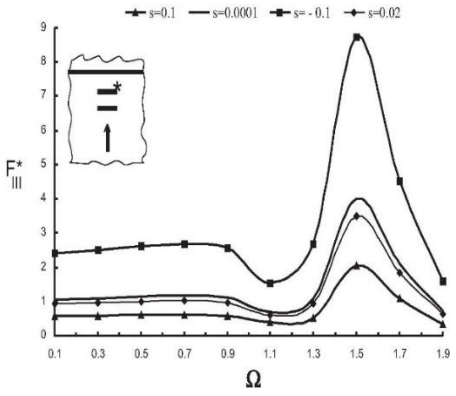

(a)

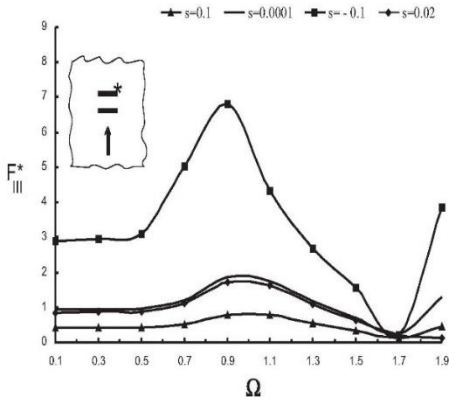

(b)

Fig. 2. Normalized SCF F_{III}^* *versus* Ω at upper nano-crack with embedded depth $d = a$ and separate distance $e = 0.5a$ from the lower nano-crack due to incident normal SH wave propagating in: (a) graded PEM half-plane with inhomogeneity magnitude $\beta = 0.2$; (b) graded PEM full plane with inhomogeneity magnitude $\beta = 0.2$. Different surface parameters *s* are used.

Figures 6a-6b clearly demonstrate that the scattered wave displacement along the traction-free surface of a graded PEM half-plane is strongly sensitive to the dynamic nano-cracks interaction and mutual nano-cracks configuration.

The obtained results have the potential to be used as a base for solution of inverse problems for identification of nano-cracks existence and their position in the functionally graded piezoelectric half-plane. All presented figures show surface elasticity effects. They appear due to the following solids state at nano-level. The number of atoms at the surface increases in respect to that in the bulk as the structural size reduces to the nanoscale. Since the surface atoms are more unstable (broken atomic bonds) than the bulk ones, they may induce the unique properties of nanomaterials.

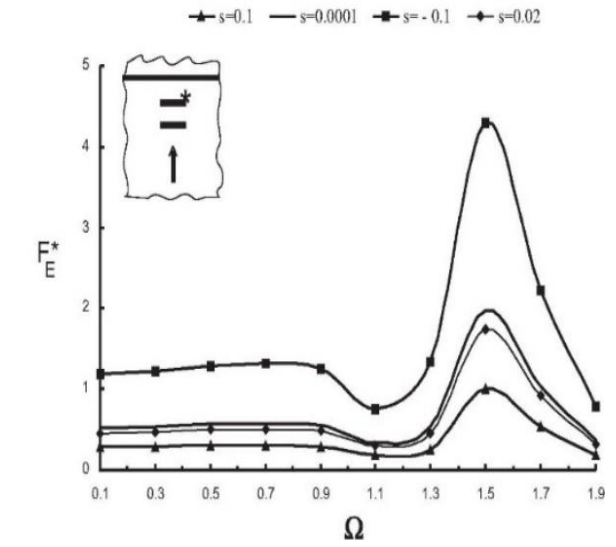

(a)

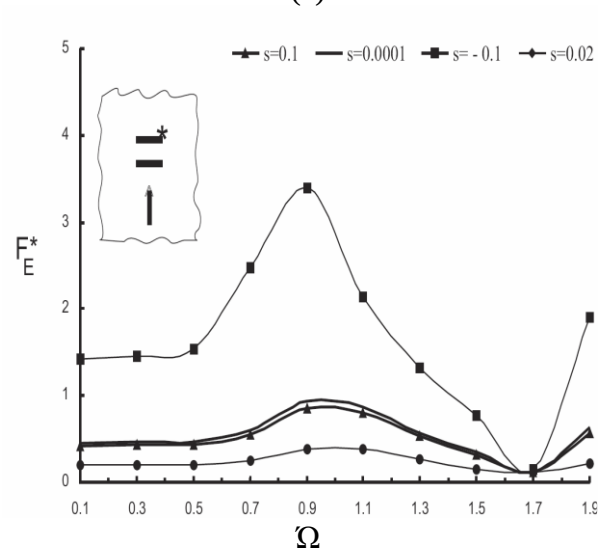

(b)

Fig. 3. Normalized EFCF F_E^* *versus* Ω at upper nano-crack with embedded depth $d = a$ and separate distance $e = 0.5a$ from the lower nano-crack due to incident normal SH wave propagating in: (a) graded PEM half-plane with inhomogeneity magnitude $\beta = 0.2$; (b) graded PEM full plane with inhomogeneity magnitude$\beta = 0.2$. Different surface parameters s are used.

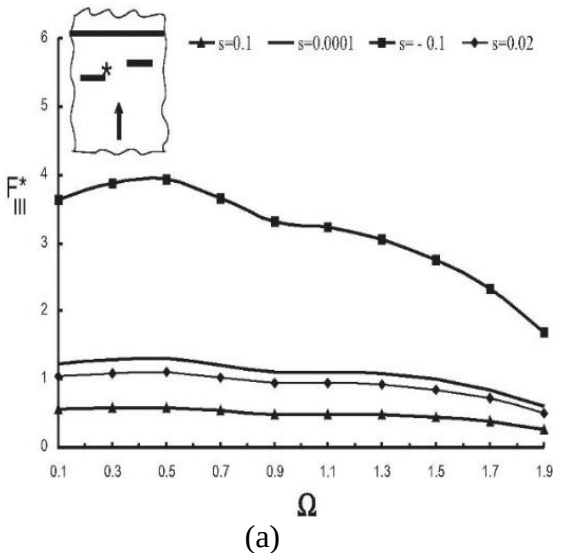

(a)

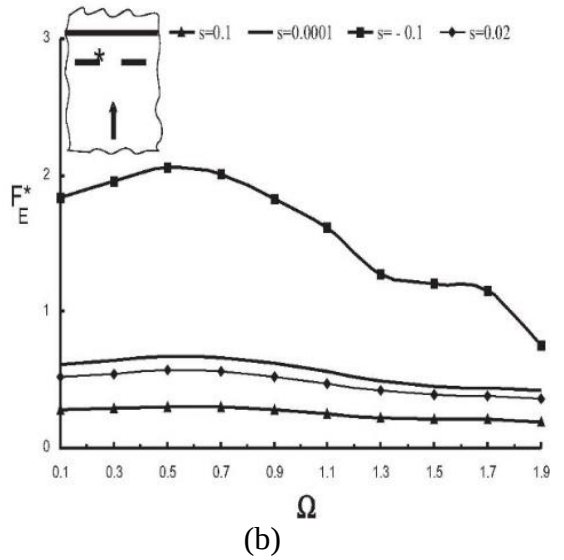

(b)

Fig. 4. Normalized mechanical F_{III}^* (a) and electrical F_E^* (b) intensity factors *versus* Ω at left nano-crack with embedded depth $d = a$ and separate distance $e = 0.5a$ from the second collinear nano-crack due to incident normal SH wave propagating in a graded PEM half-plane with inhomogeneity magnitude $\beta = 0.2$. Different surface parameters s are used.

At the nano scale, the atomic structures in the vicinity of the piezoelectric surface are far from steady. Because of the broken symmetry, they automatically modulate to be a self-equilibrated state different from those in the underlying piezoelectric bulk. The creation of an additional surface leads to excess of free energy E in the solid, i.e., the surface free energy, which is the origin of the surface effects.

CONCLUSIONS

An exponentially graded piezoelectric half-plane with two nano-cracks situated in an arbitrary mutual disposition and subjected to incident time-harmonic SH wave is studied. The computational tool is non-hypersingular traction BIEM developed in the frame of Gurtin-Murdoch model, which established the mathematical framework for incorporating surface stresses into continuum mechanics formulations.

This theory was motivated in part by empirical observations pointing to the presence of a compressive surface stress in certain types of crystals. In the Gurtin-Murdoch model, the interfaces between nano-heterogeneities and the bulk matrix are regarded as infinitely thin surfaces that possess their own deformation and surface tension characteristics. A linearized surface stress–strain constitutive relation was proposed to characterize this surface/interface effect. More specifically, the equilibrium and constitutive equations of the bulk solid are the same as those in classical elasticity, but the presence of a surface/interface stress gives rise to non-classical boundary conditions. The surface stress tensor is associated with both the bulk stress tensor and the external load by means of a force balance equation established at the solid's surface. A strong contribution is insertion of the analytically derived Green's function in the traction non- hypersingular boundary integral equations. The Green's function obeys the Sommerfeld's radiation condition and thus infinitely extended boundaries are automatically accounted for without resorting to special types of viscous boundaries as is in the domain methods such as finite difference method and finite element method. In addition, when the half-plane Green's function is used, the discretization along the free surface is avoided and as a result the size of the algebraic system is significantly reduced. The simulations conducted here illustrate that the non-uniform dynamic stress and electrical field distribution depends on the following key model factors:

(a) The incident wave characteristics;

(b) The geometry of the crack configuration and the graded half-plane boundary;

(c) The type, magnitude and properties of the material gradient;

(d) The reference material properties;

(e) The coupled material properties of piezoelectric composite materials;

(f) The surface elasticity phenomenon and the nano-crack size.

The proposed, developed and verified numerical tool has a direct application in nanomechanics and in non-destruction testing of nanomaterials.

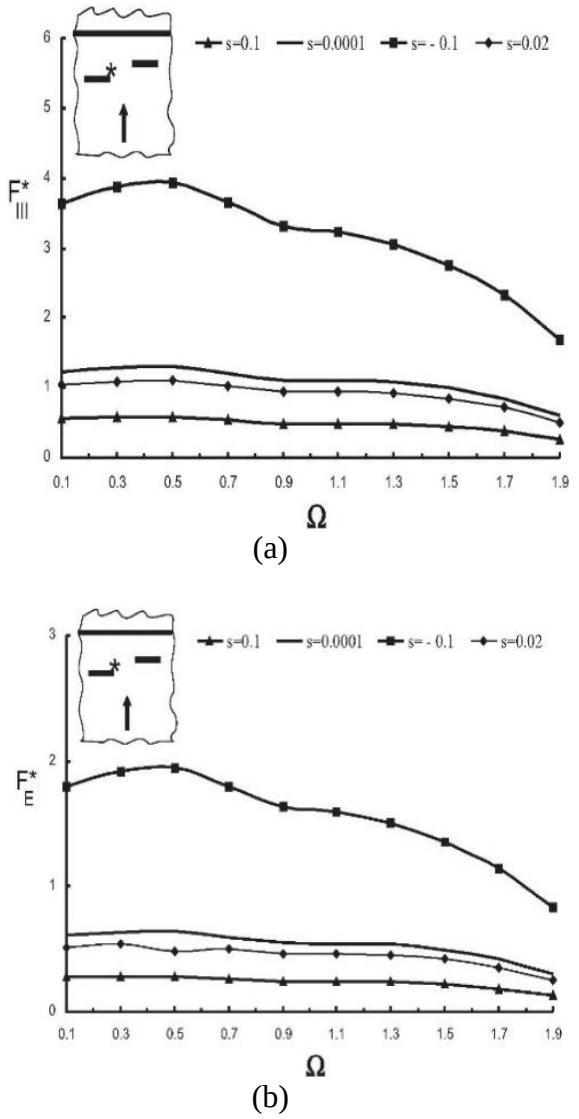

Fig. 5. Normalized mechanical F_{III}^{*} (a) and electrical F_{E}^{*} (b) intensity factors *versus* Ω at left nano-crack with embedded depth $d = a$ and separate distance $e = 0.5a$ from the second shifted nano-crack due to incident normal SH wave propagating in a graded PEM half-plane with inhomogeneity magnitude $\beta = 0.2$. Different surface parameters s are used.

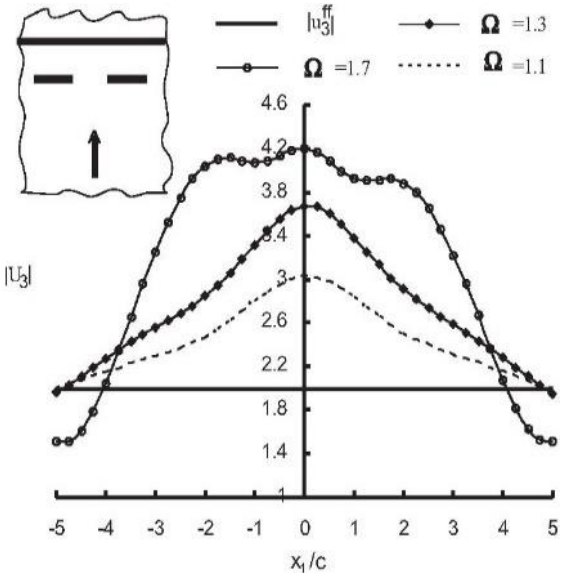

(a)

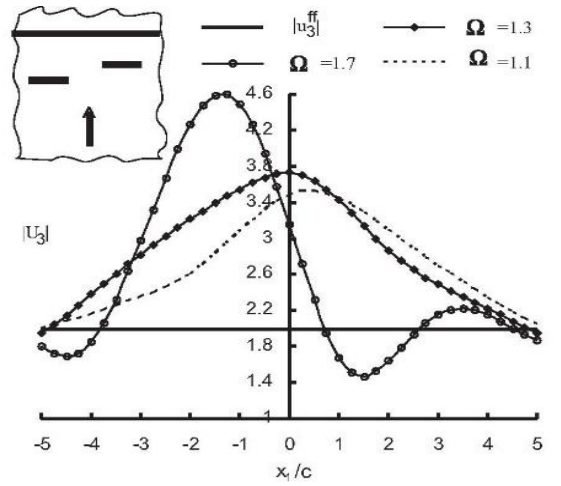

(b)

Fig. 6. Normalized displacement amplitude $|u_3|$ along the free surface of the PEM graded half-plane with the following fixed data: inhomogeneity magnitude $\beta = 0.2$, surface parameter $s = 0.02$, separate distance between both nano-cracks $e = 0.5a$, embedded depth $d = a$, frequencies of the incident normal SH wave Ω=1.1; 1.3; 1.7 for two different cracks configuration geometries: (a) two collinear nano-cracks; (b) two shifted nano-cracks.

Acknowledgement: *The authors gratefully acknowledge the Bulgarian National Science Fund for its financial support via the contract for project КП-06-Н57/3/15.11.2021.*

REFERENCES

1. R. Agrawal, B. Peng, E. Gdoutos, H. Espinosa, *Nano Lett.*, **8**, 3668 (2008).
2. F. Xu, Q. Qin, A. Mishra, Y. Gu, Y. Zhu, *Nano Res.*, **3**, 271 (2010).
3. M. Minary-Jolandan, R.A. Bernal, I. Kuljanishvili, V. Parpoil, H.D. Espinosa, *Nano Lett.*, **12**, 970 (2012).
4. G. Manolis, P. Dineva, T. Rangelov, D. Sfyris, *Engineering Analysis with Boundary Elements* (*EABE)*, **128**, 149 (2021).
5. M.E. Gurtin, A.L. Murdoch, *Archives for Rational Mechanics and Analysis*, **57,** 291 (1975).
6. T. Rangelov, P. Dineva, in: A. Slavova (ed.), NTADES, 2022, Springer PROMS, v. **412**, Springer Nature, 2023, p. 117.
7. P. Dineva, D. Gross, R. Muller, T. Rangelov, Dynamic Fracture of Piezoelectric Materials. Solutions of Time-harmonic problems via BIEM. Solid Mechanics and its Applications, v. 212, Springer Int. Publ., Switzerland, 2014.
8. Mathematica 6.0 for MS Windows. Champaign, Illinois, 2007.
9. V. B. Shenoy, *Int. J. Solids Struct.*, **39**, 4039 (2002).